Spring 2014

Pile-Soil Interaction in Unsaturated Soil Conditions

Megan Hamilton
University of New Hampshire - Main Campus

Pile-Soil Interaction in Unsaturated Soil Conditions

A Senior Honors Thesis Presented to the University Honors Program
University of New Hampshire

In Partial Fulfillment of the Requirements for Honors in Civil Engineering

By Megan Hamilton

B.S. Civil Engineering

College of Engineering and Physical Sciences

University of New Hampshire

Faculty Advisor: Dr. Majid Ghayoomi

Spring 2014

Abstract

The degree of saturation has been proven to significantly affect geotechnical engineering designs for foundations. The changes in water content will influence the way the soil behaves, including its strength and stiffness parameters. These characteristics were analyzed for a uniform silty sand by developing P-Y curves, which relate lateral loading to lateral deformations. These P-Y curves were input into FB-Multipier, a software developed by the Bridge Software Institute. The software is capable of generating deformations as a result of user-defined loading cases. The results indicated that the middle range of degrees of saturation produced the least amount of deformation. This is in accordance with stiffer response in partially saturated soils due to the presence of inter-particle suction stresses.

Table of Contents

Abstract 2
List of Figures 4
Introduction 5
Unsaturated Soil Condition 7
Soil Model 9
P-Y Curves 14
FB-Multipier 17
Results 20
Conclusions 24
Appendices 25
Appendix A: Suction Stress 25
Appendix B: P-Y Curves 26
Appendix C: FB-Multipier Instructional Report 29
References 43

List of Figures

Figure 1: Comparison of Saturated to Unsaturated Soil Conditions 7
Figure 2: Soil Model 9
Figure 3: Rate of Change of Initial Subgrade Modulus 10
Figure 4: Cylinder Pile Model 11
Figure 5: van Genuchten's Fitting Parameters 11
Figure 6: Soil Water Retention Curve (SWRC) 12
Figure 7: Suction Stress Characteristic Curve (SSCC) 13
Figure 8: P-Y Curves for Degree of Saturation = 0.20 16
Figure 9: Soil Input Dialog Box 17
Figure 10: A) Model Pile B) Displacements from Loading 18
Figure 11: Lateral Displacement Results 20
Figure 12: Effect of Degree of Saturation on Cumulative Lateral Deformation 21
Figure 13: Effect of Degree of Saturation on Partial Lateral Deformation 22
Figure 15: Lateral Deformations from 150 kN Lateral Force 23
Figure 14: Lateral Deformations from 20 kN Lateral Force 23

Introduction

Deep foundations are key elements in structural design in soft soils. They allow structures to be built upon weak or erratic soils by transferring the building load to a firm deeper soil layer. Deep foundations come in all varieties, including drilled shafts, driven piles, and caissons. Factors such as soil type, groundwater table level, and expected loads affect the selected type of foundation. Soils vary in strength and stiffness, determined based on the effective stress values. The degree of water saturation of the soil layer can change the effective stresses leading to different soil behavior. It is imperative that the variation of the degree of saturation of the site is closely studied and monitored because it may change the deep foundation response to loads, as well as the pile-soil interaction.

Driven piles are one type of deep foundations that have been commonly used because of their reliability, availability, and relatively easy construction process. They are prefabricated off-site and driven into the ground. They can vary in diameter, length, and material, which are all determined based on the given site conditions and loading. Driven piles can withstand both axial and lateral loads, as long as they are designed properly. Axial loads can induce compression or tension on the pile. The side friction and toe bearing of the pile together resist against axial loads. Lateral loads are applied perpendicular to the pile and are resisted by the lateral earth pressure.

Lateral earth pressure, which provides resistance against lateral loads, is a function of the effective stress. Thus, variation of water saturation could affect the soil lateral resistance. The pile-soil interaction is an important area of study, as it is an indicator of how well the deep foundation will perform in compliance with the surrounding soil layer. In this project, a set of

proof-of-concept analyses were performed to show the effect of partial saturation on the pile-soil interaction under lateral loading.

Unsaturated Soil Condition

Installation of deep foundations in unsaturated soil conditions presents a new set of challenges. Foundation response in unsaturated soils will vary significantly from foundation response in saturated or dry soils. Unsaturated soils are unique in that they introduce the phenomenon of suction when analyzing the soil mechanics. This suction is a result of inter-particle forces due to the presence of a three-phase material system (Figure 1). Geotechnical systems in unsaturated soil environments need to be designed with additional circumstances, such as handling flow and deformation of the soil (Alonso & Olivella 2006). These problems arise with variations in the degree of saturation. When the water content changes, it affects the suction stress which in turn will create suction gradients. These gradients have the ability to generate flow, which may be problematic when designing a geotechnical application.

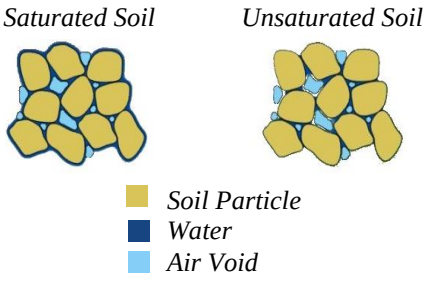

Figure 1: Comparison of Saturated to Unsaturated Soil Conditions

Stress phenomena in unsaturated soils are defined as the challenges associated in considering both the mechanical and chemical equilibrium. This includes problems with lateral earth pressure, bearing capacity, and slope stability (Lu & Likos 2004). In these cases, the parameter of interest is the soil's strength at its limit state. The other concern in unsaturated soil practice is the deformation phenomena. This is defined as the physical processes with large deformations and strains (Lu & Likos 2004). In this situation, the geotechnical engineer closely examines the moisture content of the soil. It is the changing degree of saturation that may cause

consolidation, settlement, compaction, and collapses in the soil. An example of a deformation occurrence is the shrinking and swelling of an expansive soil. A soil with these properties may cause tension cracking, heave, or pressure build up.

The change in degree of saturation and suction in unsaturated soils may vary the deformations and strength properties of the soil. In unsaturated conditions, suction stress forms a tensile strength in the soil (Lu et al. 2010). As mentioned earlier, the suction phenomena that can induce flow is known as matric suction. Matric suction is negative pore water pressures mainly above the water table. When analyzing the effective stress of a soil, the suction stress must be considered. It is essential to consider the effects of suction in deep foundation lateral analyses because changes in effective stress due to the presence of suction will influence the soil response in shallower depths, where the highest deformation occurs.

Soil Model

Since the purpose of this research was to understand and evaluate a conceptual theory, a uniform silty sand sample was chosen for simplicity (Figure 2). To eliminate variation in analysis, some soil parameters were assumed to remain constant. The internal friction angle, Φ, was assumed to be 32°. A dry unit weight, γ_d, of 18 kN/m^3 was chosen because the typical range for sands and silts is 15-23 kN/m^3 and 6-18 kN/m^3, respectively (Holtz 2011). The same tactic was applied in assuming a saturated unit weight, γ_s, of 21 kN/m^3. This parameter was used in calculating the 8specific gravity of the silty sand using Equation 1.

$$G_s = \frac{\gamma_s}{\gamma_0} \qquad \textit{Eqn. 1}$$

The void ratio in a soil, or the ratio of the volume of voids (air and/or water) to the volume of solids, was chosen from a set of a typical range of values. The void ratio, *e*, can range between 0.4-1 for sands and 0.3-1.5 for clays (Holtz 2011). For the silty sand to be analyzed, a void ratio of 0.9 was chosen, representing medium dense condition.

Figure 2: Soil Model

Other constants chosen for this soil model included the rate of change of the initial subgrade modulus, k_g, at a value of 10,000 kPa/m (Figure 3). This value comes from the assumption that the soil sample is above the water table, is a loose sample, and has a relative density of about 30%. The subgrade modulus of a soil is a strength parameter that determines the deformation from loading. By assuming that the rate of change is constant, it doesn't imply that the deformation will be the same for each layer, but instead that each layer will react at the same rate of change in deformation. Additionally, the soil was assumed to have no residual degree of saturation, S_r. Although this does not represent realistic field conditions, it will allow for a simpler and more stable numerical analysis. In reality, each degree of saturation may have different residual degrees of saturation.

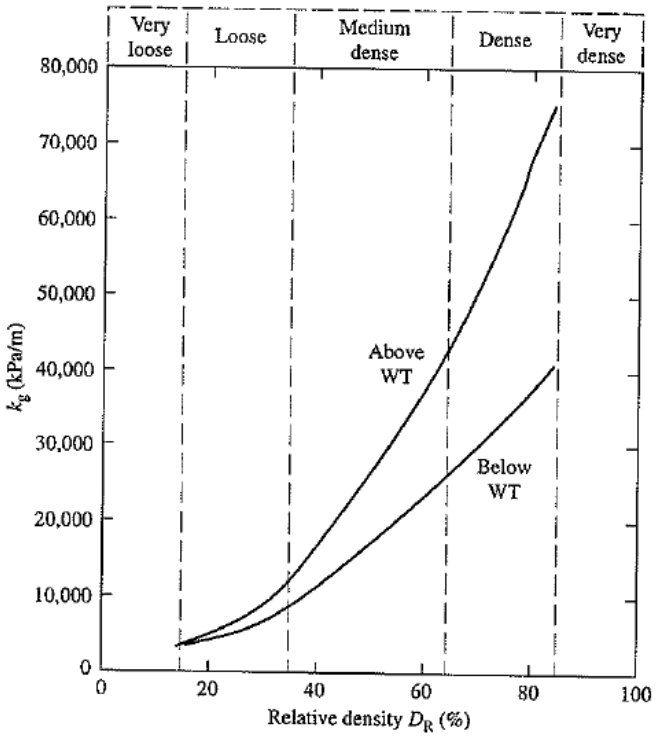

Figure 3: Rate of Change of Initial Subgrade Modulus (Salgado 2008)

The pile chosen for the analysis is a 0.25 meter diameter cylinder that is 5 meters long (Figure 4). The default reinforcement for a cylinder pile was used in analyzing the model in FB-Multipier. This reinforcement specified prestressed longitudinal bars and spirals for the shear reinforcement.

Figure 4: Cylinder Pile Model

In order to determine what points of degree of saturation should be analyzed, a soil water retention curve (SWRC) and a suction stress characteristic curve (SSCC) were first generated (Lu & Likos 2006). The degree of saturation affects both the suction and effective stress at each depth in the soil. Both the SWRC and the SSCC were produced using van Genuchten's fitting parameters (Lu et al. 2010). For silty sand, the pore size distribution parameter, *n*, ranged from

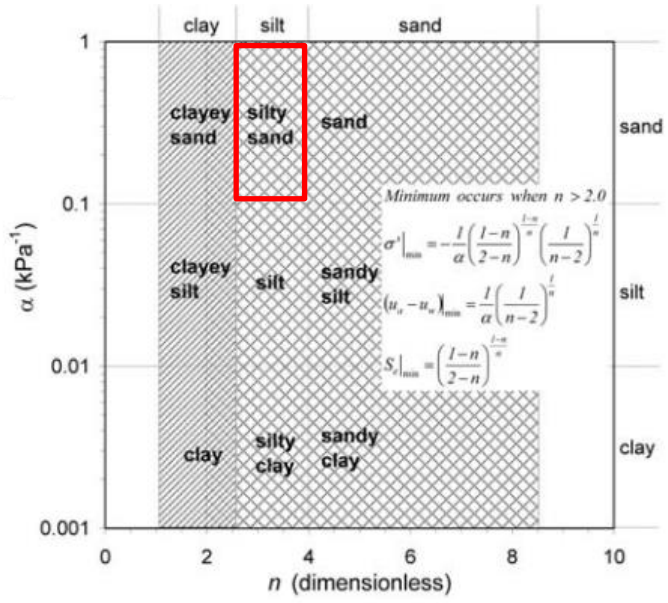

Figure 5: van Genuchten's Fitting Parameters (Lu et al. 2010)

2.5 to 4 so a value of 2.75 was chosen. The inverse of air entry value, α, ranged from 0.1 to 1 kPa^{-1}, and a value of 0.1 kPa^{-1} was chosen (Figure 5).

Van Genuchten's model for the Soil Water Retention Curve (SWRC) defined the degree of saturation as in Equation 2. The SWRC plots matric suction as a function of the degree of saturation (Figure 6).

$$S_e = \left\{\frac{1}{1+[\alpha(u_a-u_w)]^n}\right\}^{1-1/n} \qquad \textit{Eqn. 2}$$

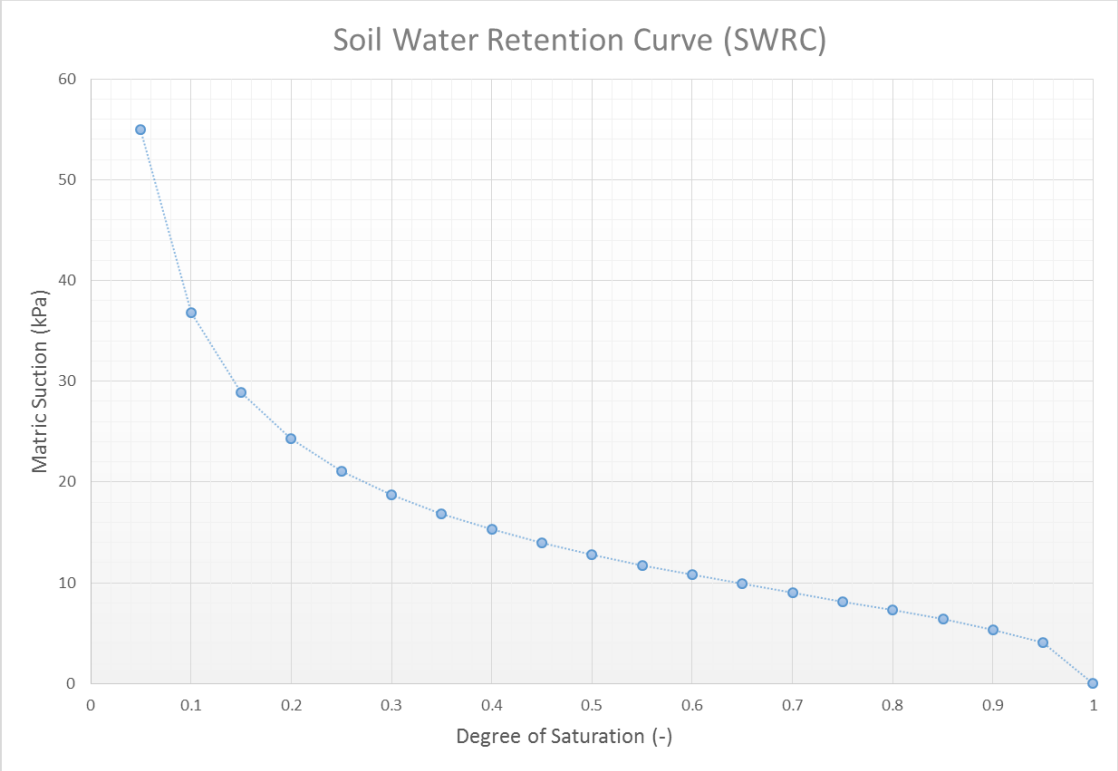

Figure 6: Soil Water Retention Curve (SWRC)

The fitting parameters, α and n, were used to obtain the suction stress in the soil using Equation 3 (Lu et al. 2010). Since it was assumed that there is no residual degree of saturation, the degree of saturation was input as the variable, S_e, defined in Equation 2. The full data set for suction stress and depth in soil for each degree of saturation can be seen in Appendix A. The

plot of degree of saturation vs. suction stress generates the suction stress characteristic curves (SSCC) (Figure 7).

$$\sigma^s = -\frac{S_e}{\alpha}(S_e^{\frac{n}{1-n}} - 1)^{\frac{1}{n}} \qquad \textit{Eqn. 3}$$

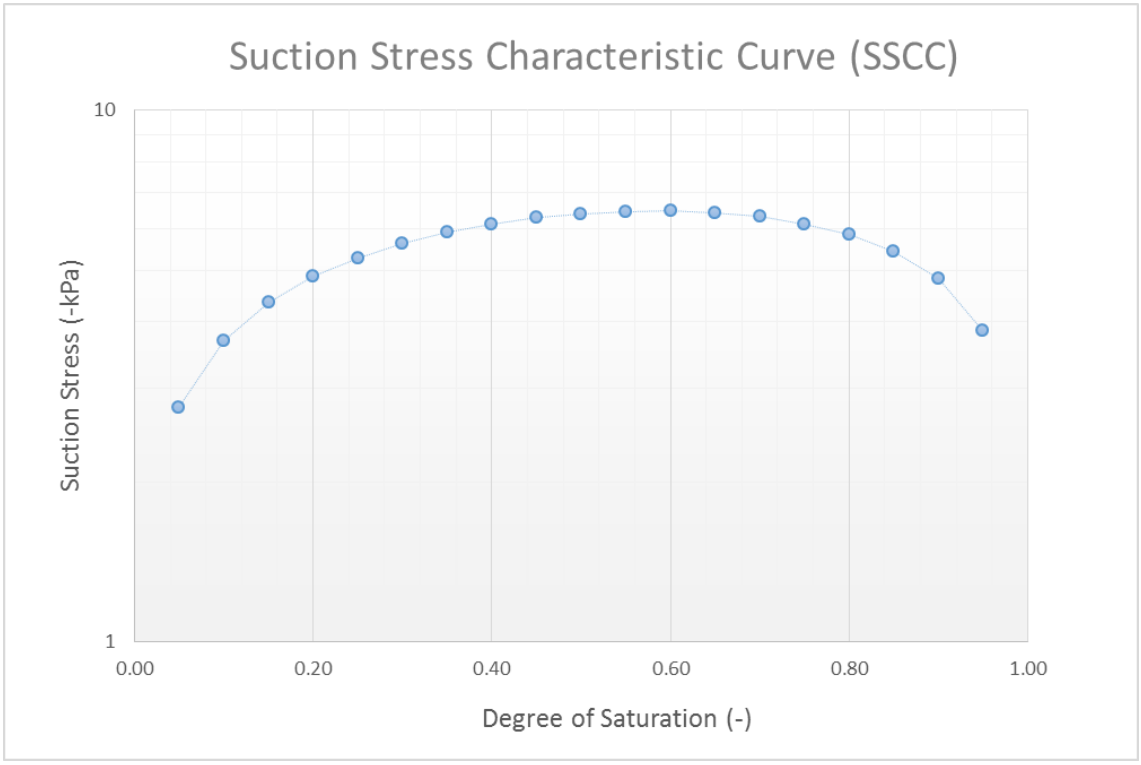

Figure 7: Suction Stress Characteristic Curve (SSCC)

From analyzing the SSCC, six degree of saturations were chosen to be analyzed. These were: 0.0, 0.20, 0.50, 0.60, 0.85, and 1.0. They were chosen based on their location on the SSCC so that the resulting data would show a wide spectrum of the effect of degree of saturation.

P-Y Curves

P-Y curves determine how specific soil parameters affect the lateral deflection of pile. They are dependent on soil type, loading, pile-soil interaction, and the depth. The first step in developing a P-Y curve is to determine the effective stress of a soil at a given depth. This analysis also assumes that the degree of saturation, and therefore the suction, remains constant with depth of soil. This is not a typical suction profile, but will allow for the effect of degree of saturation to be analyzed independently. For each six degrees of saturation chosen, an effective stress was calculated for the middle of each 1 meter thick layer of the 5 meter thick sample. Equation 4 was utilized in determining this parameter (Lu et al. 2010).

$$\sigma' = \sigma + \sigma^s \qquad \textit{Eqn. 4}$$

The next parameter needed is the limit unit resistance, p_L. This is taken as the minimum value of Equation 5 and Equation 6 (Salgado 2008). This was derived from the American Petroleum Institute (API) in 1993 and was chosen because it is the industry standard for driven piles in sand and soft clay.

$$p_L = (C_1 z + C_2 B) * \sigma'_v \qquad \textit{Eqn. 5}$$

$$p_L = C_3 B \sigma'_v \qquad \textit{Eqn. 6}$$

However, in order to use Equation 5 and Equation 6, the parameters C_1, C_2, and C_3 must first be calculated (Salgado 2008). All three are dimensionless and a function of the internal soil friction angle.

$$C_1 = 0.115 * 10^{0.0405\Phi} \qquad \textit{Eqn. 7}$$

$$C_2 = 0.571 * 10^{0.022\Phi} \qquad \textit{Eqn. 8}$$

$$C_3 = 0.115 * 10^{0.0555\Phi} \qquad \textit{Eqn. 9}$$

The API method uses Equation 10 to calculate the lateral load, *p*, in terms of many other variables including the lateral deflection, *y* (Salgado 2008). These are the two variables that will be plotted in order to develop a full P-Y curve.

$$p = Cp_L \tanh\left(\frac{k_g z y}{Cp_L}\right) \qquad \textit{Eqn. 10}$$

This equation, however, introduces a new variable, C. It can be calculated using Equation 11 (Salgado 2008).

$$C = \begin{cases} 3 - 0.8\frac{z}{B} \geq 0.9 \; for \; static \; loading \\ 0.9 \; for \; cyclic \; loading \end{cases} \qquad \textit{Eqn. 11}$$

Once all the variables in the P-Y equation are satisfied, lateral deflections of interest, *y*, can be input into the equation. The API soft clay P-Y relationships for static loading were used, where the ratio of lateral deflection to the deflection corresponding to a soil resistance of 50% of the total limit resistance, y_{50}, determines the lateral deflection, *y*, which is used in Equation 10. The variable, y_{50}, was calculated using Equation 12 (Salgado 2008). It was assumed that the axial strain corresponding to a shear stress equal to half the maximum undrained shear strength, ε_{50}, was 0.025. The variable, *B*, is the pile diameter in meters.

$$y_{50} = 2.5\varepsilon_{50}B \qquad \textit{Eqn. 12}$$

The ratio, y/y_{50}, varied from 0 to 1. From multiplying the ratio to the value of y_{50}, the lateral deflection, *y*, was calculated and used in Equation 10 to determine the value of the lateral load, *p*. Five P-Y curves were developed for each of the six degrees of saturation, one for each of the five layers of the soil. Figure 8 shows an example of five P-Y curves on the same plot, developed for

the 0.20 degree of saturation case. The P-Y curves for each degree of saturation can be found in Appendix B.

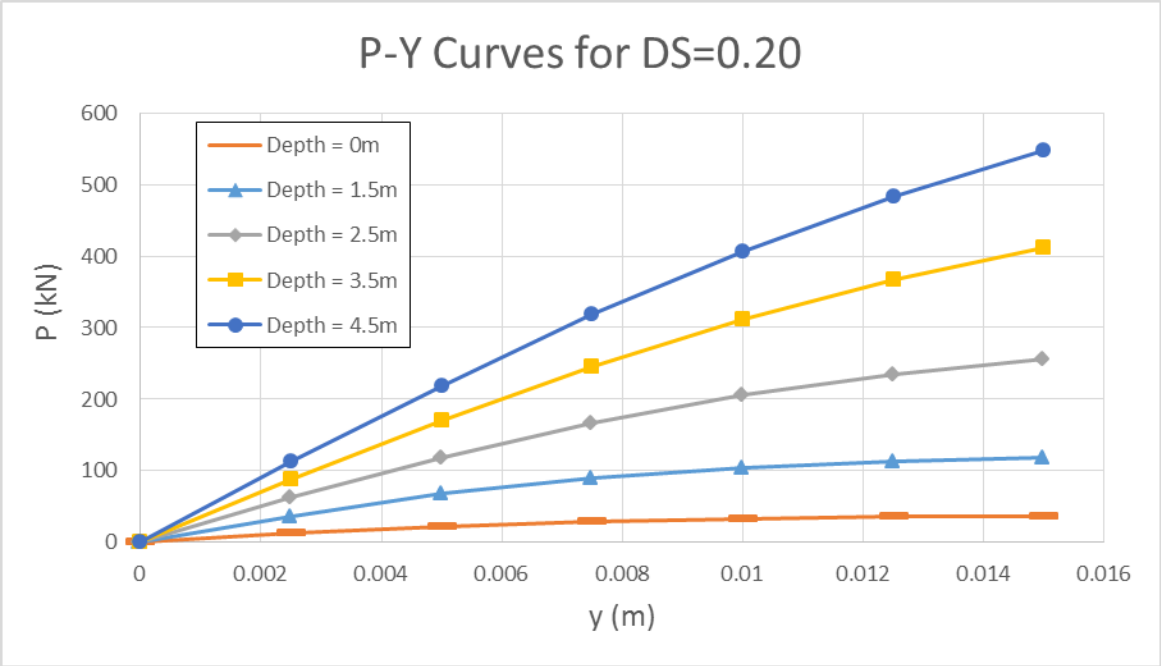

Figure 8: P-Y Curves for Degree of Saturation = 0.20

FB-Multipier

FB-Multipier is a non-linear finite element analysis program for bridge pier structures that was developed by the Bridge Software Institute (BSI), headquartered at the University of Florida. This specific software has the ability to evaluate multiple bridge pier structures under a variety of loading scenarios. The user is capable of determining many properties of the pier structure, such as type, geometry, and soil structure that it will be located in (Figure 9). The soil-pile interaction is further analyzed through the software's use of nonlinear structural finite element analysis and nonlinear static soil models for axial, lateral, and tip soil behaviors (Bridge Software Institute 2011). FB-Multipier is advantageous to an engineer because of the simplicity in which data can be directly entered into the system. It offers the engineer many opportunities to input specific data about the foundation and soil, including raw data from p-y, t-z, and q-z curves.

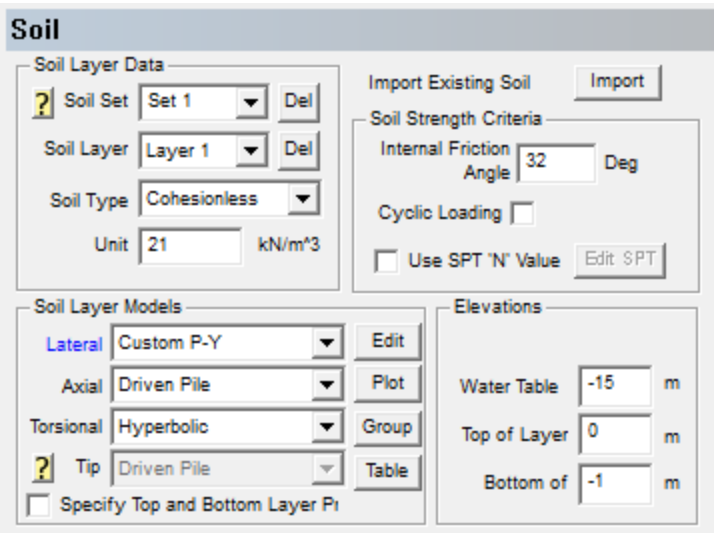

Figure 9: Soil Input Dialog Box

The specific P-Y data was input for each layer of the soil and for each degree of saturation. This feature allows the user to input data that is very specific to the project they are

analyzing. It is a more accurate option than choosing one of the pre-determined methods, such as O'Neill's, Reese's, or API's methods.

Once all the soil properties were determined and assigned to the soil layers, a load case was applied. Each pile was subjected to a 100 kN lateral force, y_p, and a 10 kN axial force, z_p. The model of the pile before any loading can be seen in Figure 10(A) and the resulting deformations for each degree of saturation is shown in Figure 10(B).

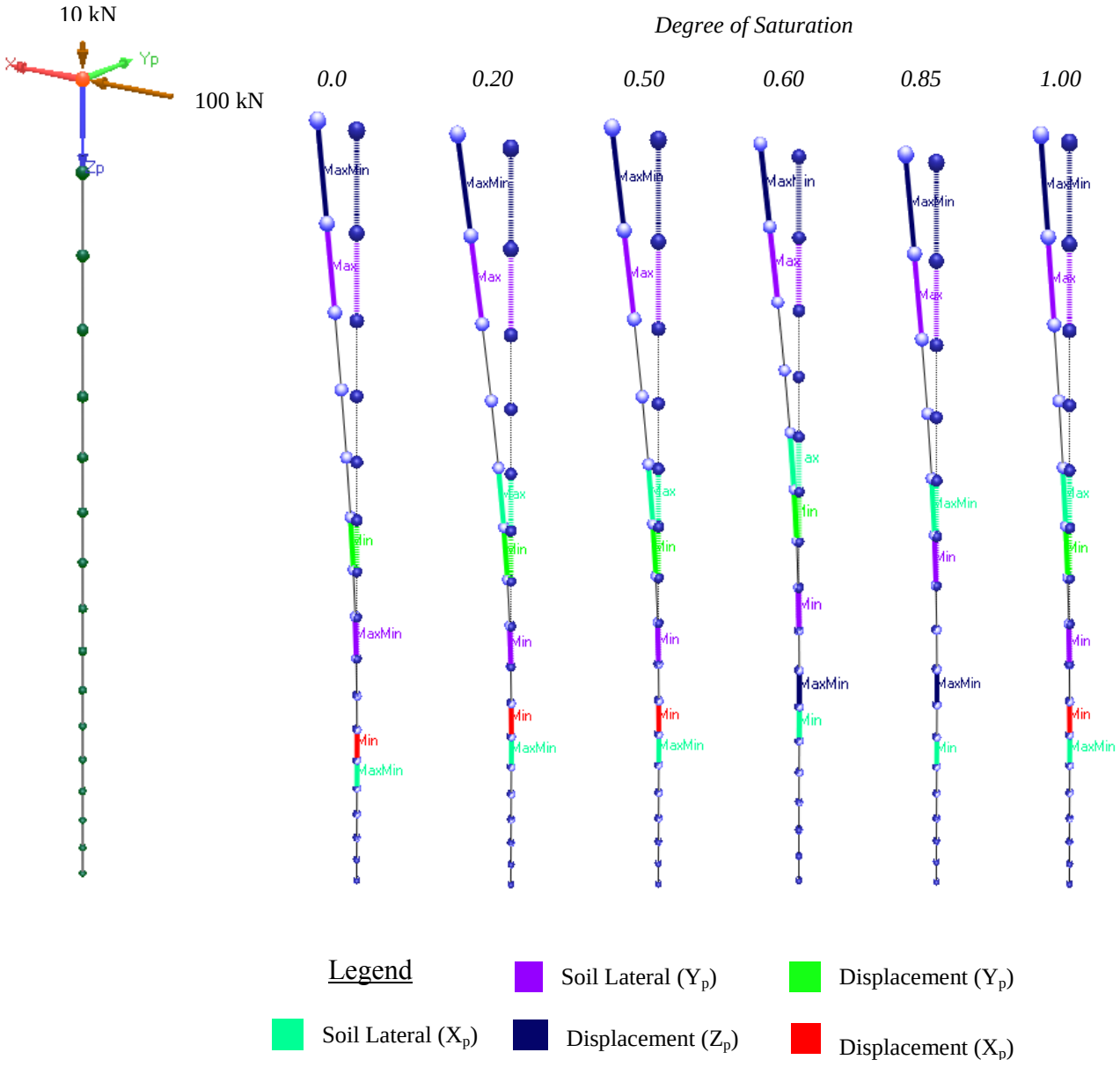

Figure 10: A) Model Pile B) Displacements from Loading

As shown in Figure 10(B), FB-Multipier also has the ability to show the location of the maximum and minimum displacements due to the induced loading. Each case was run as a static analysis, where the pile behaved nonlinearly. The static analysis means that a permanent load is applied and the structure is allowed to reach static equilibrium between stiffness and displacement. In the nonlinear analyses, FB-Multipier used the custom stress strain curves to apply to the entire cross-section of the pile. For these tests, P-delta and P-Y moments are used for analysis. Both moments take into account the effect of the axial force; P-delta moments look at the deflection of both ends of a member, whereas the P-Y moments will analyze the internal displacements of a member. For further reference on FB-Multipier, an instructional report can be found in Appendix C.

Results

As shown in Figure 10, FB-Multipier returned results of maximum and minimum soil and pile displacements. These results correspond well with the original SWRC and SSCC. Figure 11 shows the effect of the degree of saturation on lateral displacement.

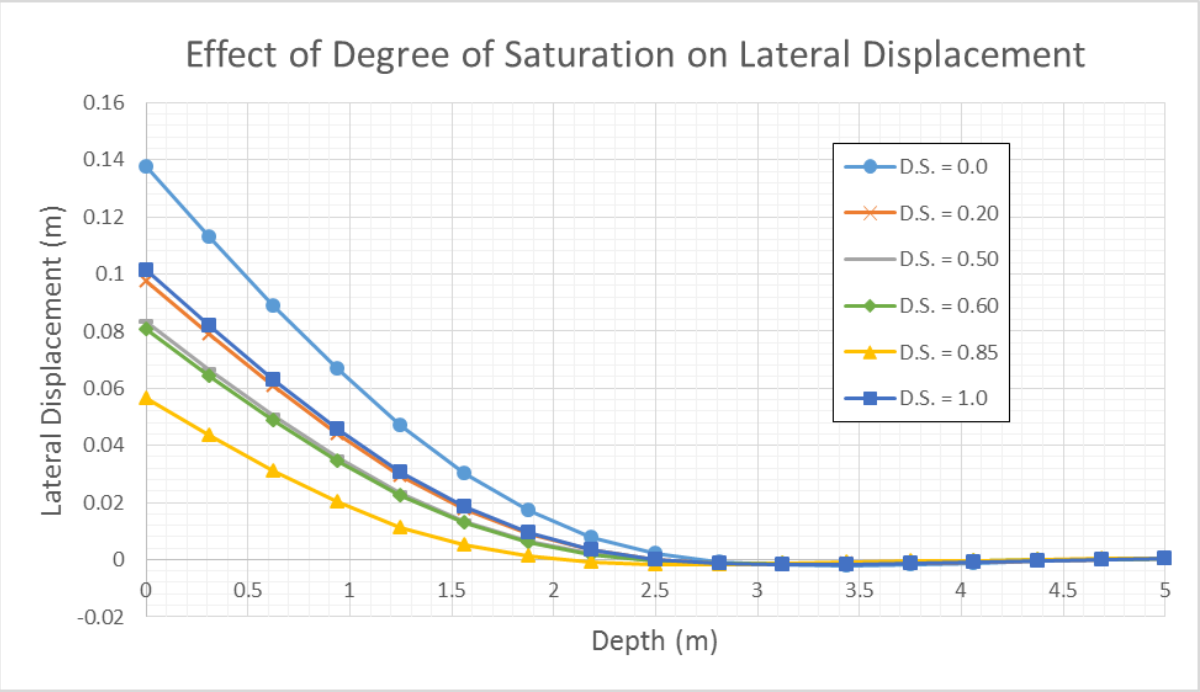

Figure 11: Lateral Displacement Results

The light blue and dark blue lines represent the degrees of suction of 0.0 and 1.0, respectively. The rest of the lines, which show lateral displacements less than those of 0.0 and 1.0, prove that the middle range of suction results in greater stiffness. This is because the middle range of suction (0.20, 0.40, 0.60, and 0.85) have greater effective stress in the soil, therefore causing the least amount of deformation. This correlates with the SSCC because these points also have greater suction stresses. The increased suction stress will contribute to the soil's stiffness, as it provides the tensile resistance in the soil.

The results from FB-Multipier also reported that the maximum axial displacement (Z_p) and lateral soil displacement (Y_p) occur closer to top of pile. This is reasonable because that is where the axial and lateral loads were applied to the pile, as well as where the maximum moment occurred. Also, the minimum pile and soil lateral displacements occurred at the bottom of pile.

A normalized plot, relative to the dry condition, of the effect of the degree of saturation on cumulative lateral deformation is shown in Figure 12. Four depths were chosen to model: 0.0 m, 0.63 m, 1.5 m, and 3.44 m. From this plot, it is noticeable that the effect of suction is greater at depths closer to the top of the pile. The depth of 1.5 m shows the least amount of cumulative deformation, but once the depth exceeds 1.5 m, the lateral deformation increases. Due to higher significance of suction stress in overall effective stress in shallower depth, the pile is stronger and able to resist deformation closer to the top of the pile.

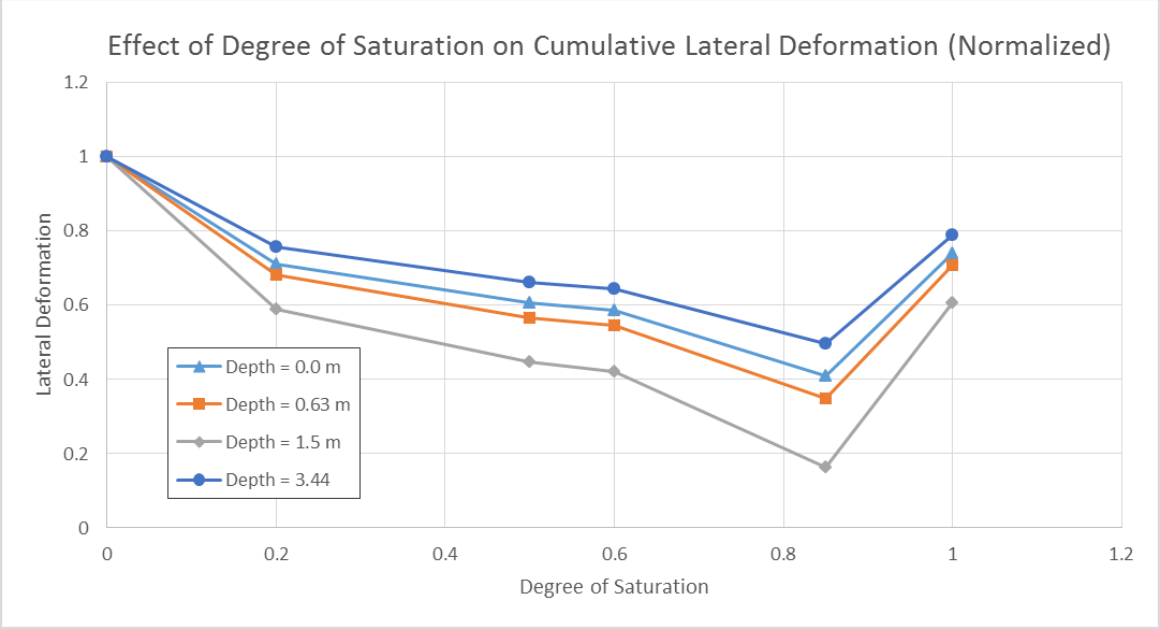

Figure 12: Effect of Degree of Saturation on Cumulative Lateral Deformation

Figure 13 shows the normalized plot for the effect of the degree of saturation on partial lateral deformation. This graph shows the same trend as Figure 12, where the depth exceeding 1.5 m shows the greatest lateral deformation. This graph was altered so that only the deformation specific to the depth would show. It does not take into account the previous deformations of the pile, as Figure 12 did.

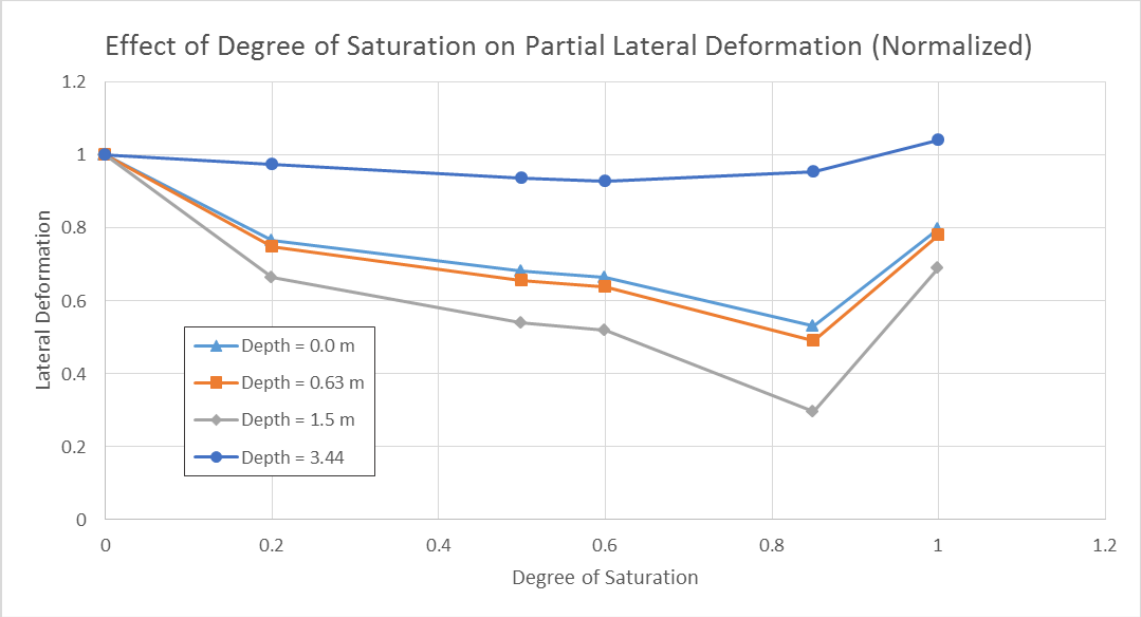

Figure 13: Effect of Degree of Saturation on Partial Lateral Deformation

The pile also underwent two additional lateral loadings, one at 20 kN and one at 150 kN. Figure 14 shows the resulting lateral deformations from replacing the 100 kN applied lateral force with 20 kN. Figure 15 shows the results from replacing the applied lateral force with 150 kN.

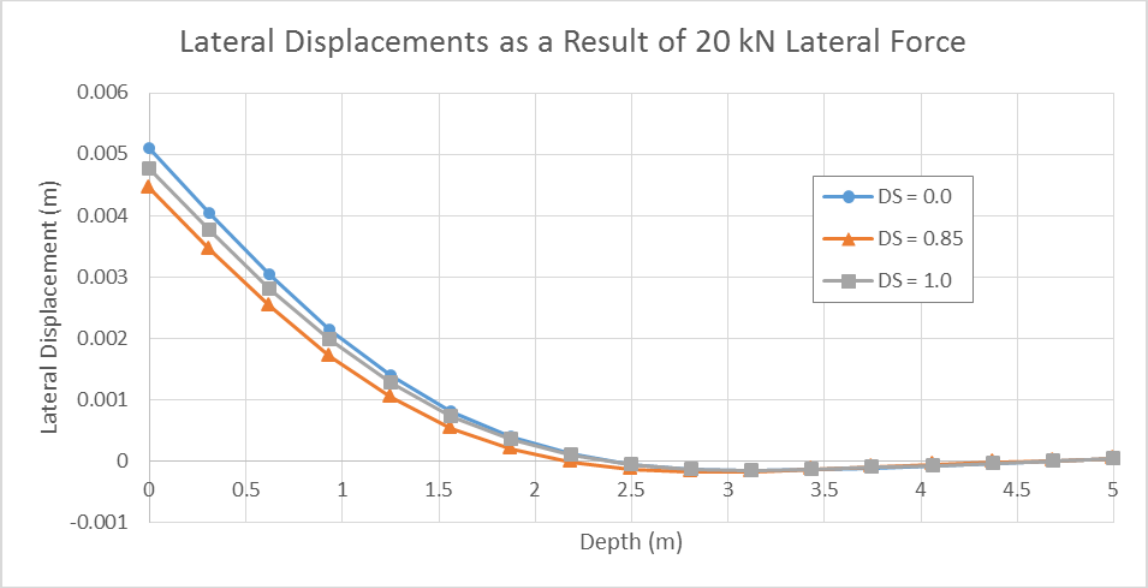

Figure 15: Lateral Deformations from 20 kN Lateral Force

As expected, the degree of saturation has the same effect on the lateral deformation in both cases. It is important to note that both extreme cases of saturation (wet and dry) result in the greatest lateral deformation because it is when the soil is the weakest. Additionally, it is notable that the 150 kN lateral force has a more significant impact on the lateral deformation. This force resulted in lateral deformations with a range of 0.17 m to 0.41 m for the three degrees of saturation, whereas the range for the 20 kN force was only 0.004 m to 0.005 m.

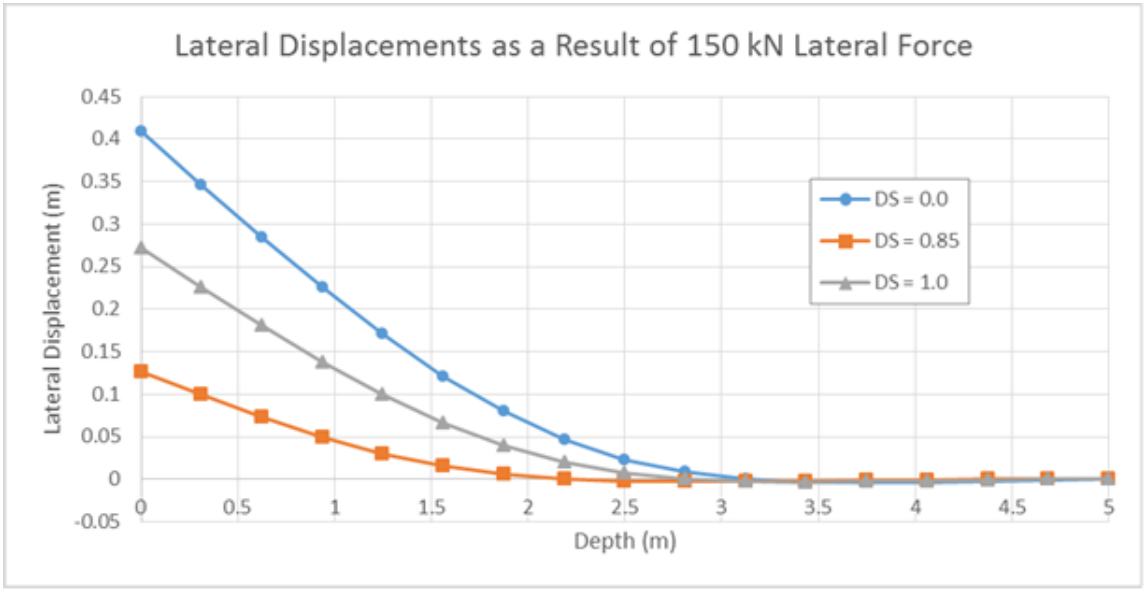

Figure 14: Lateral Deformations from 150 kN Lateral Force

Conclusions

The objective of this study was to determine how the degree of saturation affects the soil-pile interaction in deep foundations. Unsaturated soils are an important field of study, especially in foundation engineering, because the changing degree of saturation can greatly influence the soil behavior.

The degrees of saturation of interest were chosen off a suction stress characteristic curve after soil properties, such as effective stress and suction stress were determined. A P-Y curve was developed for each layer of soil at each degree of saturation. These P-Y curves were input into the software FB-Multipier in order to receive deformation information of the pile. These results were analyzed to see how the degree of saturation affected the deformations.

It was found that the least amount of deformation occurred in the middle range of saturation. This is because the effective stress is greatest when it is not at either extreme of the saturation range. The difference is that the soil-pile response was more pronounced in shallower ground where the suction values are considerable in overall effective stresses. The model pile as also subjected to two additional lateral loadings: 20 kN and 150 kN. These results agreed with the previous ones and showed that at greater applied lateral forces, the range of deformation is greater.

Overall, the degree of saturation is a parameter that engineers should take the time to study and understand as it relates to a specific design project. It is imperative to know field conditions, especially the degree of saturation, before the design process begins. It is also the engineer's responsibility to design a cost-effective, yet conservative option.

Appendices

Appendix A: Suction Stress

Table 1: Suction Stress for each Degree of Saturation

Degree of Saturation		σ^s	ρ_w	γ_w
(decimal)	(%)	(-kPa)	Mg/m^3	kN/m^3
0.00	0.00	0.00	1.80	17.66
0.05	5.00	2.76	1.84	18.03
0.10	10.00	3.69	1.88	18.40
0.15	15.00	4.35	1.91	18.77
0.20	20.00	4.87	1.95	19.14
0.25	25.00	5.28	1.99	19.51
0.30	30.00	5.62	2.03	19.89
0.35	35.00	5.90	2.06	20.26
0.40	40.00	6.12	2.10	20.63
0.45	45.00	6.29	2.14	21.00
0.50	50.00	6.40	2.18	21.37
0.55	55.00	6.46	2.22	21.74
0.60	60.00	6.47	2.25	22.11
0.65	65.00	6.42	2.29	22.49
0.70	70.00	6.31	2.33	22.86
0.75	75.00	6.12	2.37	23.23
0.80	80.00	5.84	2.41	23.60
0.85	85.00	5.43	2.44	23.97
0.90	90.00	4.82	2.48	24.34
0.95	95.00	3.86	2.52	24.71
1.00	100.00	0.00	2.56	25.08

Appendix B: P-Y Curves

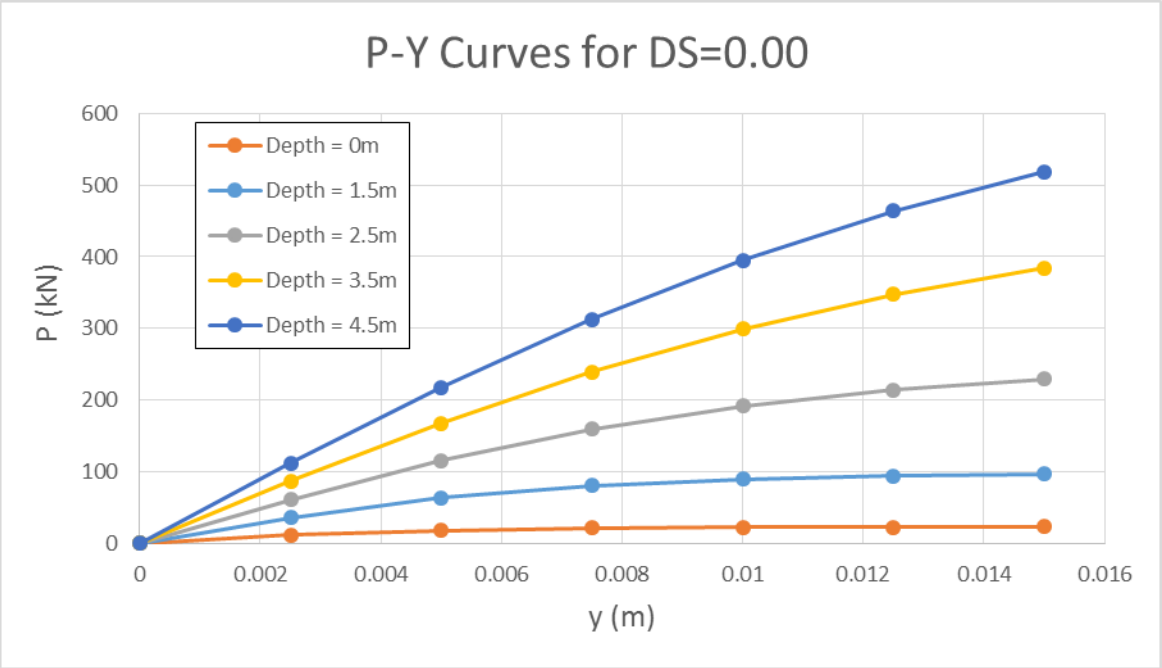

Figure A 2: P-Y Curves for Degree of Saturation = 0.00

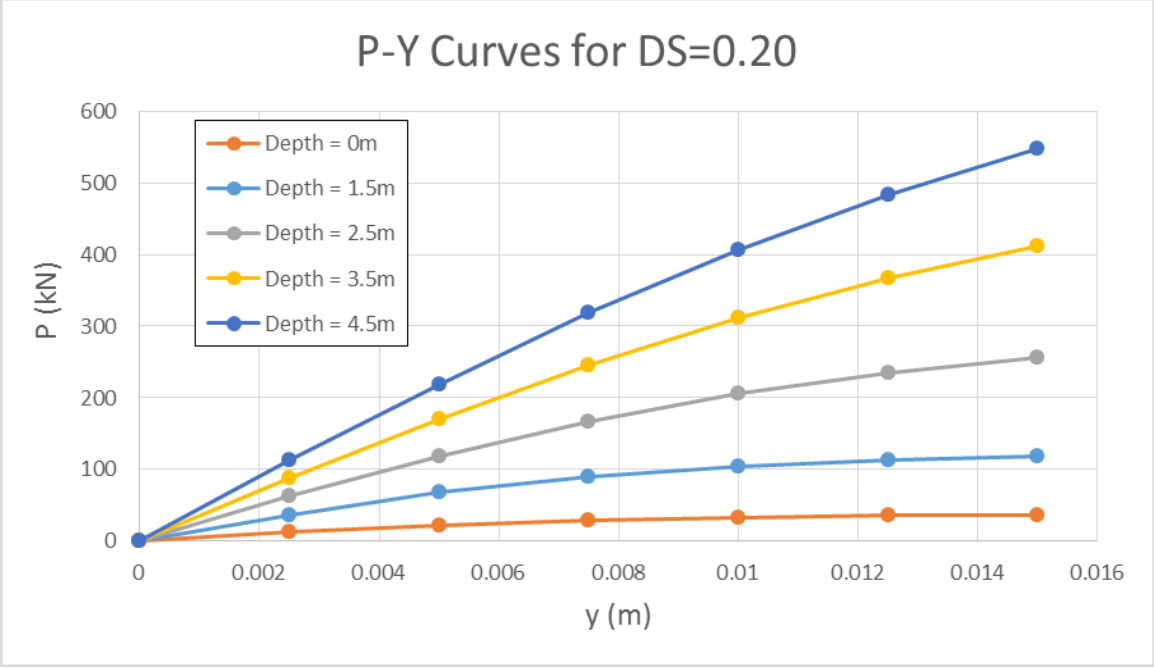

Figure A 2: P-Y Curves for Degree of Saturation = 0.20

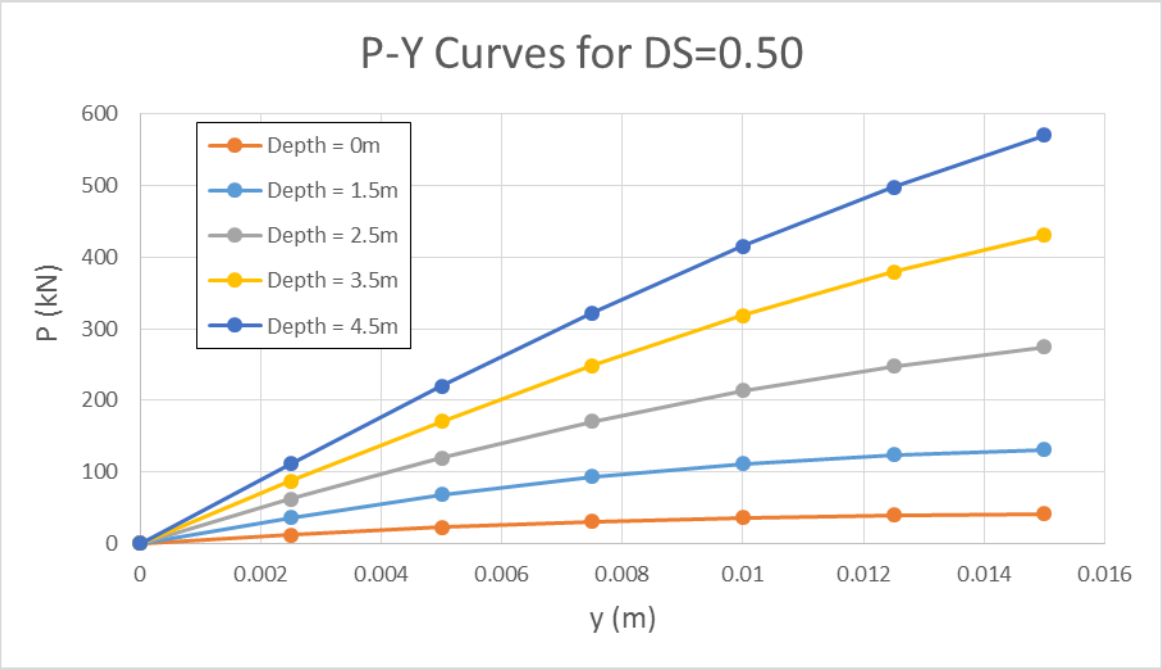

Figure A 4: P-Y Curves for Degree of Saturation = 0.50

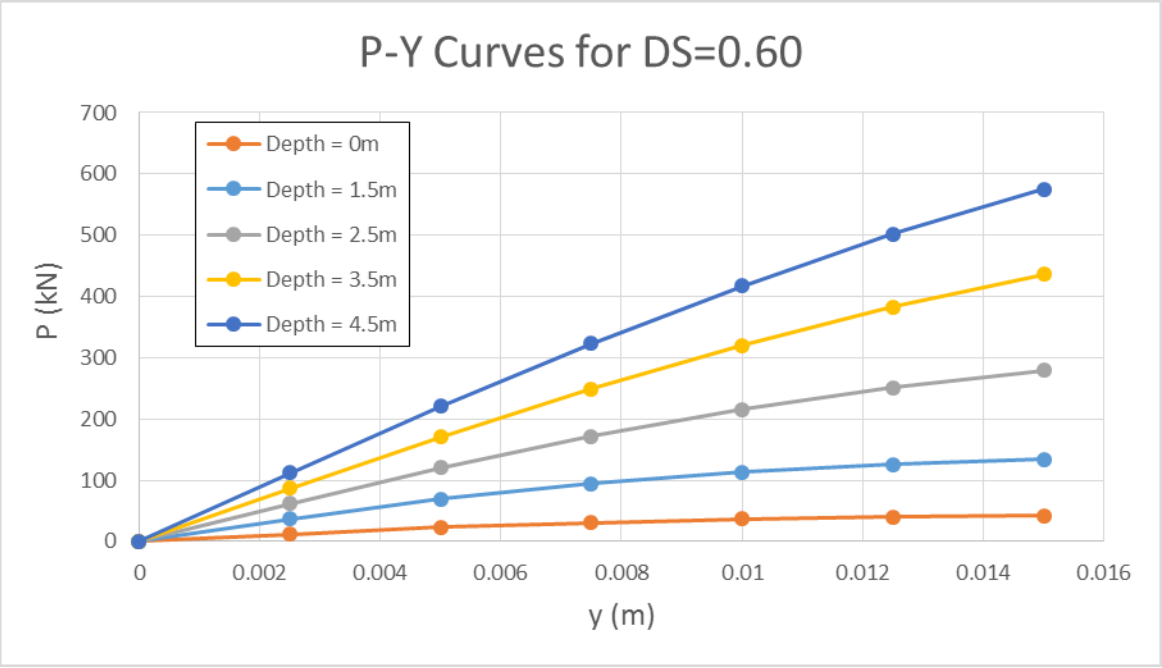

Figure A 4: P-Y Curves for Degree of Saturation = 0.60

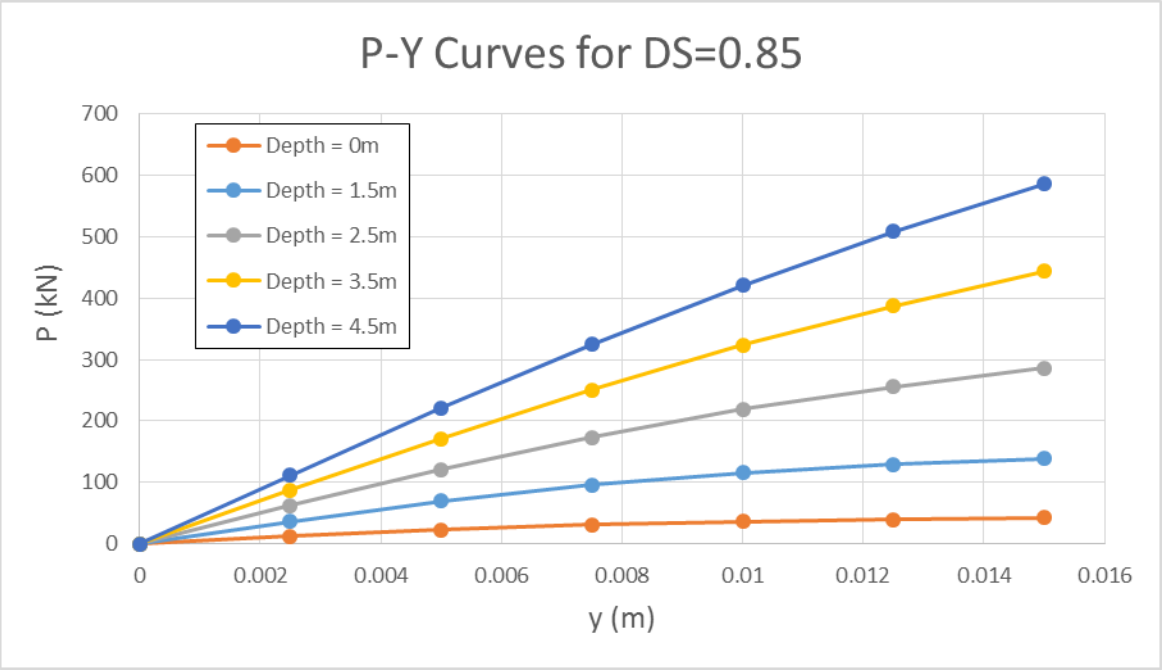

Figure A 6: P-Y Curves for Degree of Saturation = 0.85

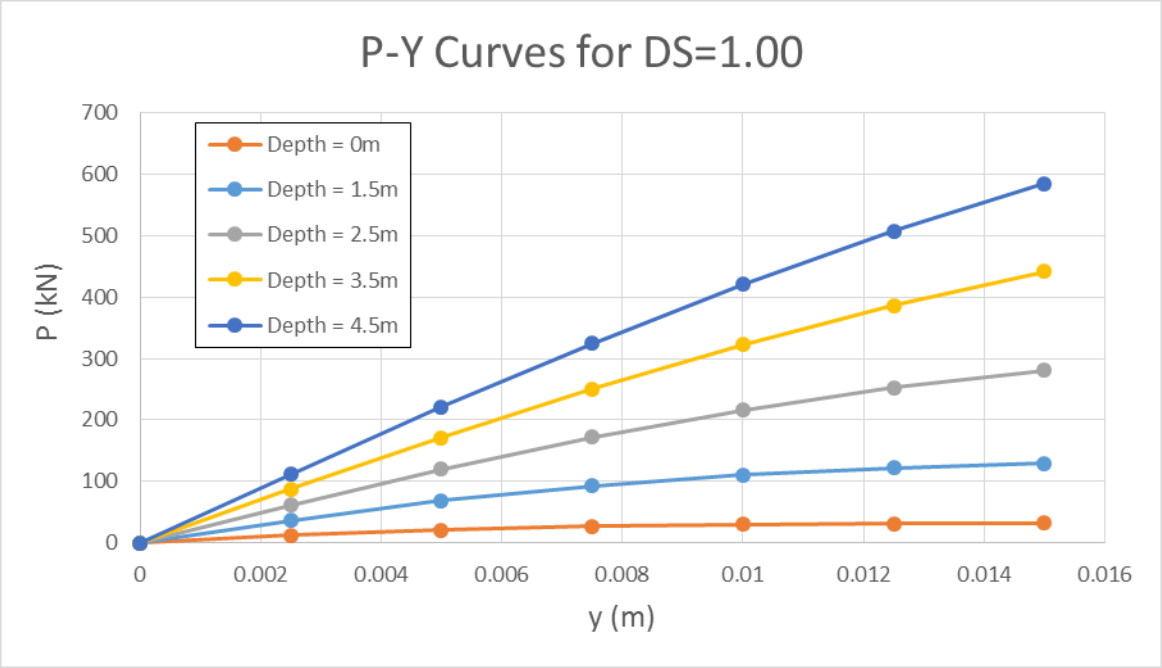

Figure A 6: P-Y Curves for Degree of Saturation = 1.00

Appendix C: FB-Multipier Instructional Report

Overview

FB-Multipier is a non-linear finite element analysis program for bridge pier structures that was developed by the Bridge Software Institute (BSI). This specific software has the ability to evaluate multiple bridge pier structures under a variety of loading scenarios. The user is capable of determining many properties of the pier structure, such as type, geometry, and soil structure that it will be located in. The soil-pile interaction is further analyzed through the software's use of nonlinear structural finite element analysis and nonlinear static soil models for axial, lateral, and tip soil behaviors (Bridge Software Institute 2011). FB-Multipier is advantageous to an engineer because of the simplicity in which data can be directly entered into the system. It offers the engineer many opportunities to input specific data about the foundation and soil, including raw data from p-y, t-z, and q-z curves.

Analysis

In all the cases of types of foundation that the user can choose, FB-Multipier always has the option of whether the pile or pier will behave linearly or non-linearly. If the user chooses linear behavior, the software will assume that the pier or pile will be purely linearly elastic and that the deflections caused from loadings will not cause secondary moments. Secondary moments are also known as area moment of inertias, as they can predict bending or deflection in the structure (The Engineering Toolbox). However, if nonlinear behavior is deemed appropriate, then the software will either use a custom or default stress strain curve to apply to the cross-section of the pile being designed. In nonlinear behavior, P-delta and P-y moments are used for analysis. Both moments take into account the effect of the axial force; P-delta moments look at

the deflection of both ends of a member, whereas the P-y moments will analyze the internal displacements of a member.

FB-Multipier is able to analyze a structure both statically and dynamically. In static analysis, a permanent load is applied and the structure reaches static equilibrium between the stiffness and displacement. The dynamic loading analysis, however, is a bit more complicated. Within a dynamic analysis, the user can choose between time-step integration and a modal response model. Time step integration refers to the implicit integration that is used to solve results at every time step. This method allows for structural analysis in the cases where damping and inertial effects are considered to be significant. Equation 1 is used in determining the structural response to external loading.

$$F(t) = M\ddot{x} + C\dot{x} + Kx \qquad \textit{Eqn. 1}$$

Where: M = mass matrix, $\ddot{x}$ = nodal acceleration vector, C = damping matrix, $\dot{x}$ = nodal velocity vector, K = stiffness matrix, x = nodal displacement vector, and F(t) = external force vector

In modal response analysis, static loads are applied and then the software performs response spectrum analysis, meaning that the maximum force and displacement values are approximated from the model. FB-Multipier features a dynamic relaxation function that is used to stage loading in a transient dynamic analysis. In this method, the software initializes the dynamic system so that it is in equilibrium with a set of static loads, such as gravity, and is deemed as F_p. In the dynamic relaxation feature, equation 2 is used to model motion.

$$F(t)_0 + F_P = M\ddot{x}_0 + C\dot{x}_0 + K_{st}x_{st} \qquad \textit{Eqn. 2}$$

Where: M = constant, $\ddot{x}_0$ = initial nodal acceleration vector, C = constant, $\dot{x}_0$ = initial nodal velocity vector, K_{st} = stiffness matrix from static pre-analysis, x_{st} = nodal displacement vector from static pre-analysis, and $F(t)_0$ = initial transient load vector

One of the key advantages of using the dynamic relaxation feature is that it uses the software to account self-weight into the loading for dynamic structural analysis. Figure 1 shows a model of a single 30" x 30" square prestressed pile that was analyzed using static analysis, dynamic analysis with instantaneous gravity loading, and dynamic analysis with static pre-analysis (the dynamic relaxation method as previously discussed).

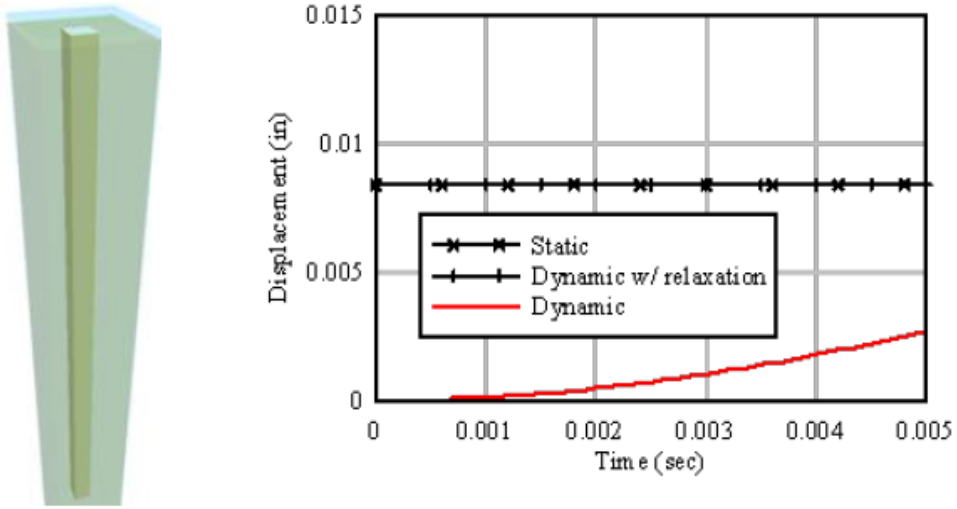

Figure 1: Displacements of Single Pile using Three Analysis Methods (Bridge Software Institute)

In this example, the vertical displacements were measured from the pile head. It is evident to see that the dynamic relaxation analysis output is directly on top of the static analysis.

After analysis, the user can choose to view three interaction diagrams: biaxial moment, two axes, and three axes. The user can select an individual pile, pile segment, or pile element to see its interaction diagram. The option to input a custom phi value, or choose to let the software use the default one, is given in the model data window. Figure 2 shows an example interaction diagram for a pile segment, in terms of biaxial moment.

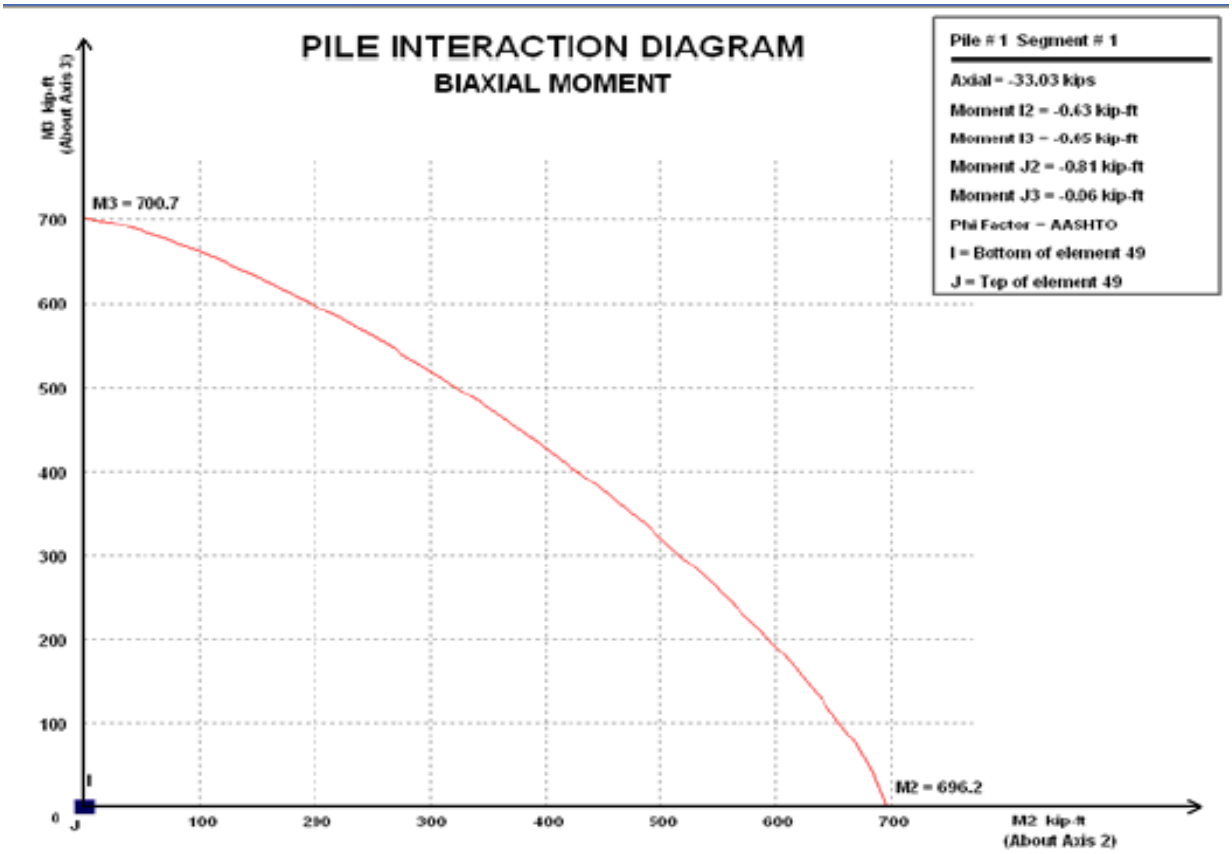

Figure 2: Interaction Diagram for a Pile Segment (Biaxial Moment) (Bridge Software Institute)

FB-Multipier will also provide a data table with the points on the interaction diagram, as shown in Figure 3. The software also creates an interaction diagram for the uniaxial model, seen in Figure 4.

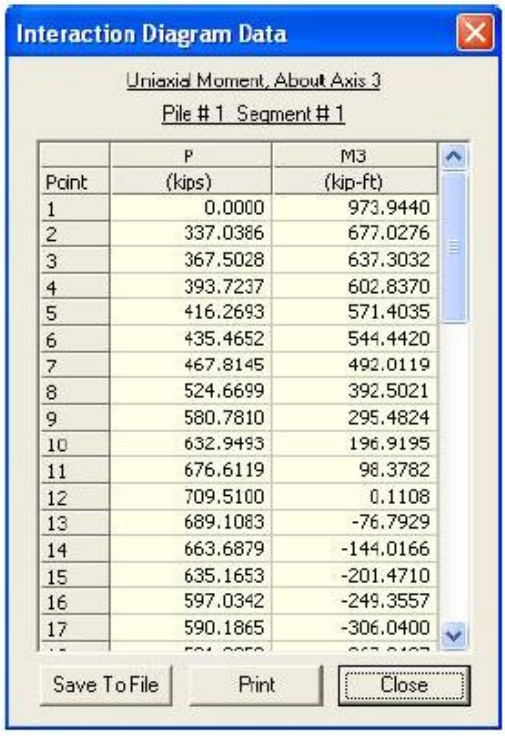

Point	P (kips)	M3 (kip-ft)
1	0.0000	973.9440
2	337.0386	677.0276
3	367.5028	637.3032
4	393.7237	602.8370
5	416.2693	571.4035
6	435.4652	544.4420
7	467.8145	492.0119
8	524.6699	392.5021
9	580.7810	295.4824
10	632.9493	196.9195
11	676.6119	98.3782
12	709.5100	0.1108
13	689.1083	-76.7929
14	663.6879	-144.0166
15	635.1653	-201.4710
16	597.0342	-249.3557
17	590.1865	-306.0400

Figure 3: Interaction Diagram Data
(Bridge Software Institute)

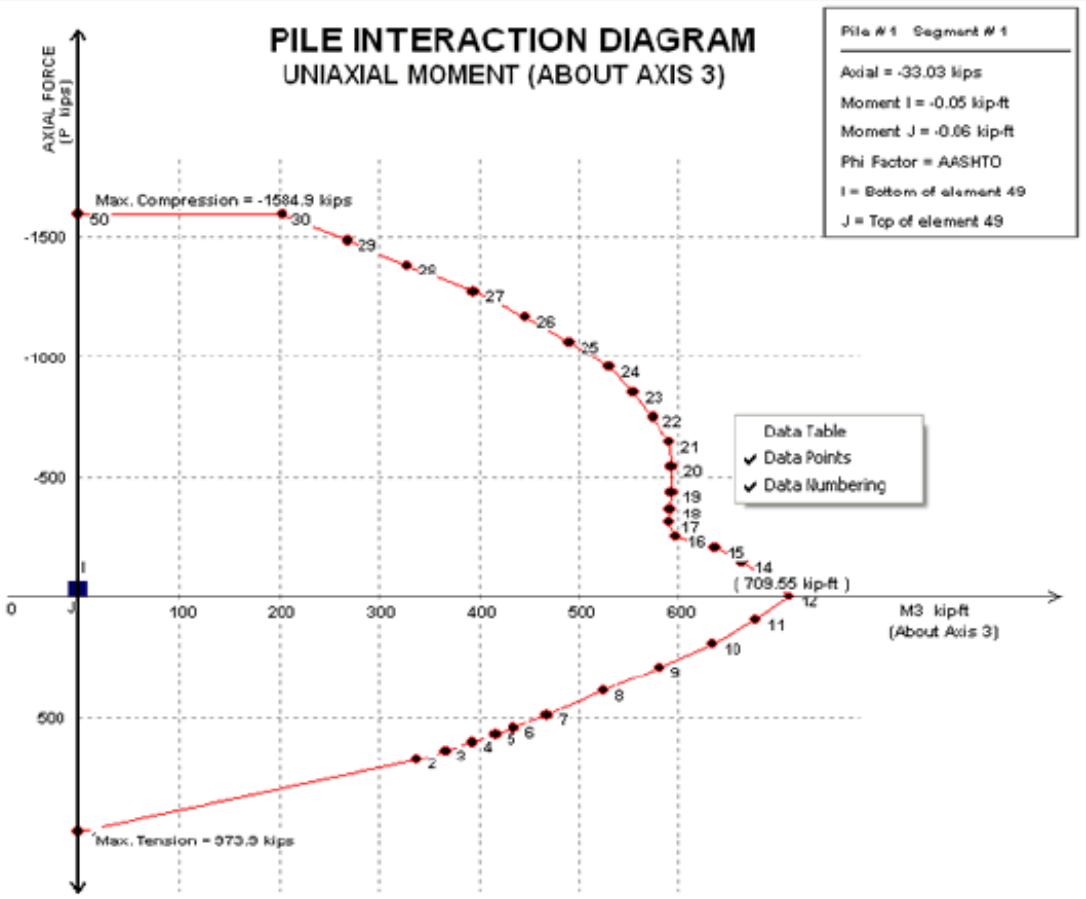

Figure 4: Interaction Diagram for a Pile Segment (Uniaxial Moment)
(Bridge Software Institute)

Soil Modeling

In FB-Multipier, the user has the capability to create soil sets and layers to accurately model the field conditions of the pier or pile. The soil layer models that are available to model are lateral, axial, and tip. Within these soil layer models, the types of soil that can be specified include cohesionless, cohesive, and rock.

The first soil layer model, lateral, offers four different models for cohesionless analysis. These include: sand (using O'Neill's method), sand (using Reese method), sand (using API method), and a custom P-Y method (user-defined method). The O'Neill method for cohesionless analysis, derived in 1984, uses equation 3 to recommend a p-y curve for the sand.

$$p = \eta A p_u \tanh\left[\left(\frac{kz}{A\eta p_u}\right) y\right] \qquad \textit{Eqn. 3}$$

Where: η= factor used to describe pile shape; A=0.9 for cyclic loading and 3-0.8z/D≥0.9 for static loading; D=diameter of pile; p_u=ultimate soil resistance per unit of depth; k=modulus of lateral soil reaction; z=depth; y=deflection

If choosing to use the O'Neill method, the user must input the modulus of lateral soil reaction (k) and the angle of internal soil friction (Φ), which may be obtained from an insitu standard penetration test (SPT). Before the O'Neill method was derived, Reese, Cox, and Koop developed p-y curves for static and cyclic loading of sands in 1974. Their theory was based on sands that underwent extensive testing of pipe pile in Texas. To use this method, the user must supply the angle of internal friction (Φ), the subgrade modulus (K), and the sand's effective unit weight (γ'). Figure 5 shows the comparison of the O'Neill and Reese methods. It should be noted that the curves fit initially, but then differ as the ultimate soil resistance (p_u) also differs.

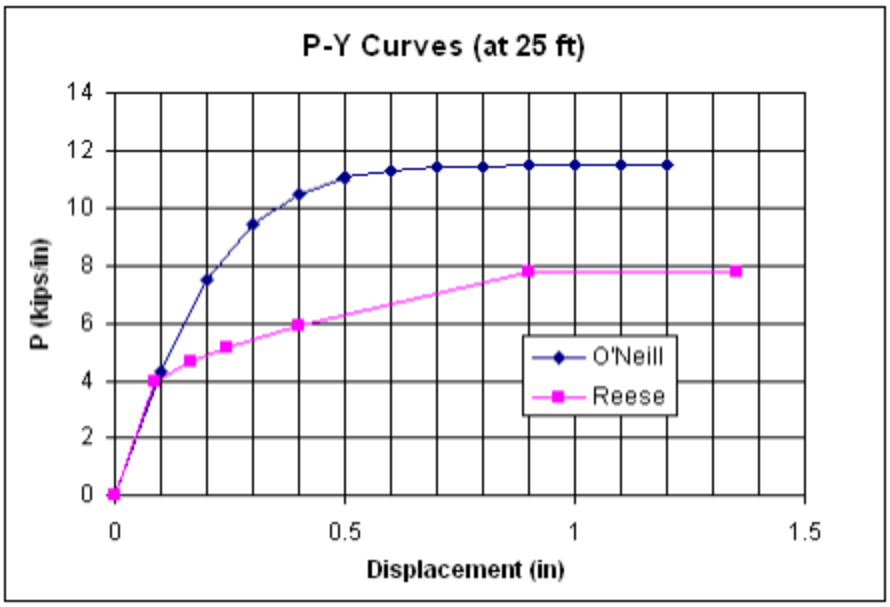

Figure 5: Comparison of O'Neill's and Reese's P-Y Curves (Bridge Software Institute)

Another method available is the American Petroleum Institute's (API) derivation. It differs from the O'Neill method in that the ultimate lateral bearing capacity for the sand at a given depth is chosen as the minimum between two equations. It is, however, similar to O'Neill's method in that the lateral soil resistance-deflection (p-y) relationship can be modeled with equation 4, using the same variables as O'Neill's.

$$P = Ap_u \tanh\left(\frac{kz}{Ap_u} y\right) \qquad \textit{Eqn. 4}$$

Finally, the user also has the opportunity to input a custom p-y curve using their own data. It is a simple option if there is specific data to the field conditions that one is designing for.

If the user desires to model cohesive soil, this also has many methods that are represented. The first one they can choose is O'Neill's method for static and cyclic loading of clays. If this option is chosen, then the user must supply the clay's undrained strength (c), strain at 50% failure (ε_{50}) and 100% (ε_{100}) failure from an unconfined compression test. If the field conditions specify that the clay will be soft clay below the water table, then the user should

choose this option that models the clay after Matlock's p-y representation from 1970. In this case, the user must supply soil unit weight (γ), undrained strength (c), and the strain at 50% failure (ε_{50}) in an unconfined compression test. Alternatively, if the clay below the water table is stiff, then this too can be modeled using the method derived by Reese et al. in 1975. In this option, the user must provide the soil's subgrade modulus (k), unit weight (γ), undrained strength (c), strain at 50% failure (ε_{50}) in unconfined compression test, and the average undrained strength (c_{avg}) for the whole clay layer. These methods would be inapplicable to clay above the water table; however there is an alternative for this situation. Reese and Welch's p-y model for stiff clays above the water table from 1975 is used by the program. For this option, the user would need to input the soil unit weight, undrained strength, strain at 50% failure stress in an unconfined compression test, and the average undrained strength for whole clay layer. This model is a function of number of load cycles, which FB-Multipier would take into account. If the user desires to model the clay using the API method, then FB-Multipier will use a series of equations to determine the ultimate lateral bearing capacity (p_u) of the soft clay under static lateral loads. FB-Multipier uses values for the equations that are recommended for the Gulf of Mexico clays. As it was with cohesionless soils, the user still has the option to input their own p-y curve data to create a more accurate representation.

Rock can be modeled in three different ways in FB-Multipier: as limestone (McVay), limestone (McVay, no 2 -3 rotation), and as custom P-Y. In the McVay limestone option, the data for the p-y curves is based on the report "Development of Modified T-Z curves for large diameter piles/drilled shafts in limestone for FBPIER" (McVay et. al 2004). In this report, lateral load tests were performed in a centrifuge with varying diameters, embedments, and rock strengths. From these tests, the data was used to back calculate the P-Y curves. The average of

these curves was used for FB-Multipier. The user also has the option to use the McVay method for limestone, but without 2-3 rotation, meaning that the pile rotation about 2 and 3 axes are not accounted for. This method does not consider the effect of side shear on the shaft. FB-Multipier cautions the user if this option is chosen, so that the appropriate p-y curve is used in analysis.

Similarly to the lateral soil model, the axial soil layer model also offers four different options for cohesionless soil: driven pile, drilled shaft in sand, driven pile in sand using API method, and custom. In the case of a driven pile, FB-Multipier uses an equation to model the pile-soil interaction along the length of the pile. It is assumed that the side springs are highly nonlinear in this model. The user has to input the initial shear modulus of soil (G_i), the Poisson's ratio of soil (v), and the maximum shear stress between the pile and soil at the given depth (T_f). For a drilled shaft in sand, the T-Z curves recommended by Wang and Reese (1993) are used. As shown in Figure 6, nonlinear springs were used to compute immediate settlements of a drilled shaft in sand.

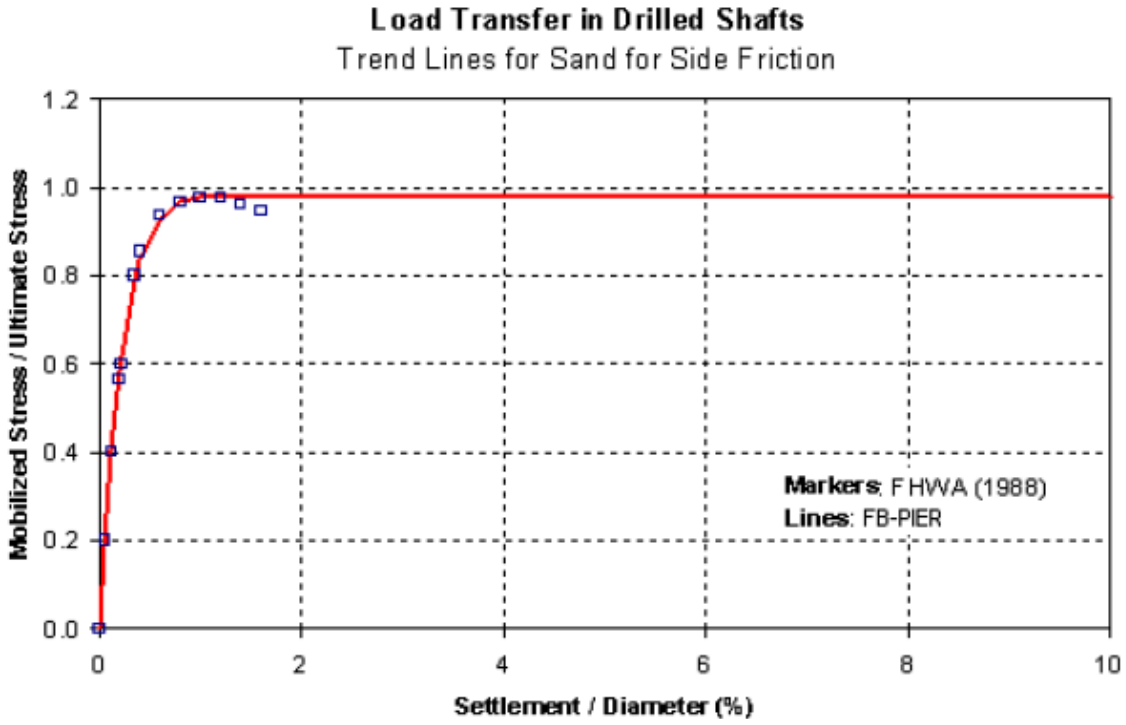

Figure 6: Drilled Shaft Side Friction in Sand
(Bridge Software Institute)

For a driven pile in sand, equation 5 is used to calculate the unit skin friction.

$$f = Kp'_0 \tan(\delta) \qquad \textit{Eqn. 5}$$

Where: K=coefficient of lateral earth pressure, p'_0=effective overburden pressure, and δ=friction angle between soil and pile wall

FB-Multipier uses a piecewise linear function to analyze the limiting values of the unit skin friction. Finally, the user has the option to insert their own data set of T-Z curves.

The analysis for a driven pile in cohesive soil is represented by the same equation used for cohesionless soil. However, in the case of a drilled shaft in clay, the analysis is a little different. Figure 7 shows the trend line for the side friction of a drilled shaft in clay. It is similar to the trend line for a drilled shaft in sand, although it is noticeable that the FHWA and Multipier data points seem to overlap more.

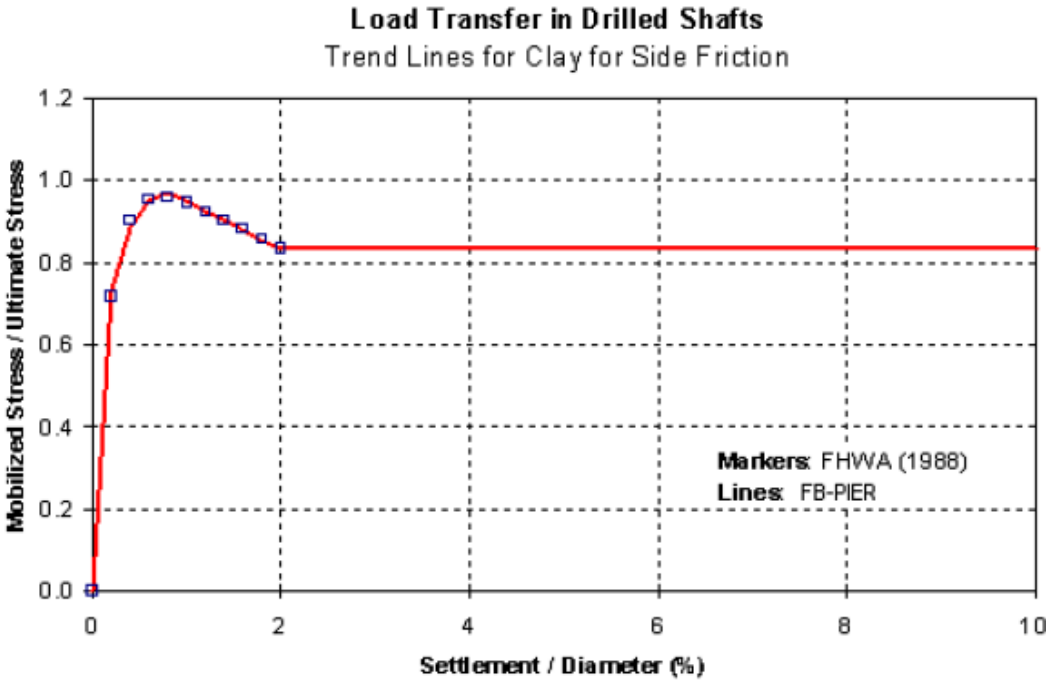

Figure 7: Drilled Shaft Side Friction in Clay
(Bridge Software Institute)

For a driven pile in clay using the API method, equation 6 is utilized in determining skin friction.

$$f = \alpha c \qquad \textit{Eqn. 6}$$

Where: α= dimension-less factor defined through a series of equations based on ψ and

c=undrained shear strength of the soil

If the user needs to model a pile or shaft in rock, they have four options: a driven pile, a drilled shaft in intermediate geomaterial (IGM), a drilled shaft in limestone, and custom. As it was the case with cohesionless and cohesive soil, the model for a driven pile in rock is the same equation. However, if it is a drilled shaft in IGM, FB-Multipier will follow FHWA's Load Transfer for Drilled Shafts in Intermediate Geomaterial. Intermediate geomaterial includes materials such as heavily overconsolidated clay, calcareous rock, and very dense granular geomaterials. In order to use this option, the required data is rather lengthy. Examples include the soil unit weight, number of layers, drilled shaft diameter, the Young's modulus of the drilled shaft, and the concrete parameters. If the drilled shaft is located in limestone, then the software uses the T-Z curves from McVay et. al (2004). In these tests, the load that was applied to the top of a drilled shaft was converted into shear stress on the rock-shaft interface. In this option, the ultimate unit skin friction values were estimated from the horizontal tangents of the T-Z curves.

When modeling the tip resistance for an element, the user has many options between drilled shaft or driven pile, and sand, clay, or IGM. In the case of a driven pile, equation 7 is used.

$$z = \frac{Q_b(1-v)}{4r_0 G_1[1-\frac{Q_b}{Q_f}]^2} \qquad \textit{Eqn. 7}$$

Where: Q_f = ultimate tip resistance, G1 = initial shear modulus, v = Poisson's ratio, r0 = radius of pile or shaft, Q_b = mobilized tip resistance

For a driven pile in sand using the API method, FB-Multipier calculates the unit end bearing, the bearing capacity factor, and the ultimate end bearing capacity. The q-z curves are then produced using a piecewise linear function and are show in Figure 8.

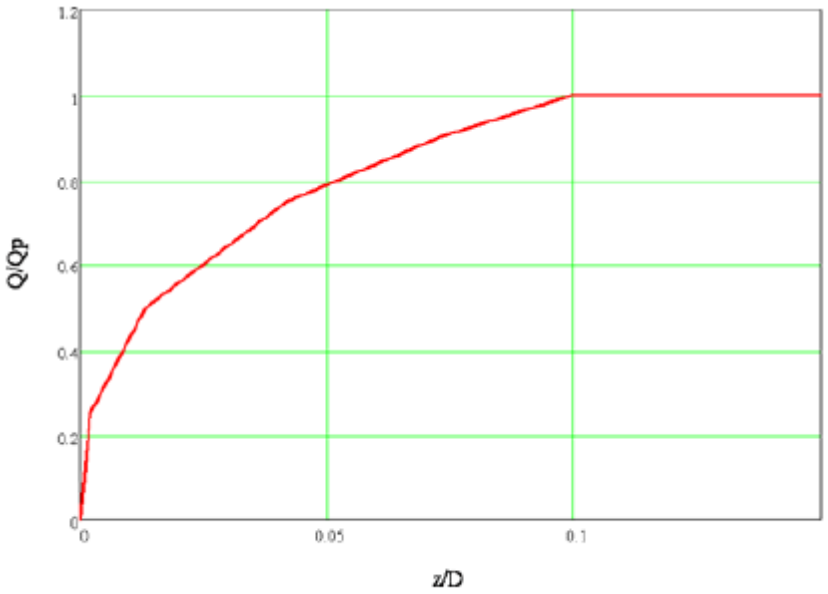

Figure 8: q-z Curve for Driven Pile in Sand (API)
(Bridge Software Institute)

If the driven pile is located in clay, FB-Multipier will calculate the unit end bearing of the pipe pile. For this, the user needs to input the undrained shear strength of the soil. The unit end bearing of the pipe pile is then used to calculate the ultimate end bearing capacity, given that the user provides the cross sectional area at the tip of the pile. For drilled shafts, the options of soil modeling include: sand, clay, and IGM. All of these options are based on Wang and Reese (1993). The trend lines for drilled shaft end bearings in sand is shown in Figure 9 and similarly, the trend lines for end bearings in clay are shown in Figure 10. In both cases, it is evident how the FHWA and FB-Multipier trend lines are nearly identical.

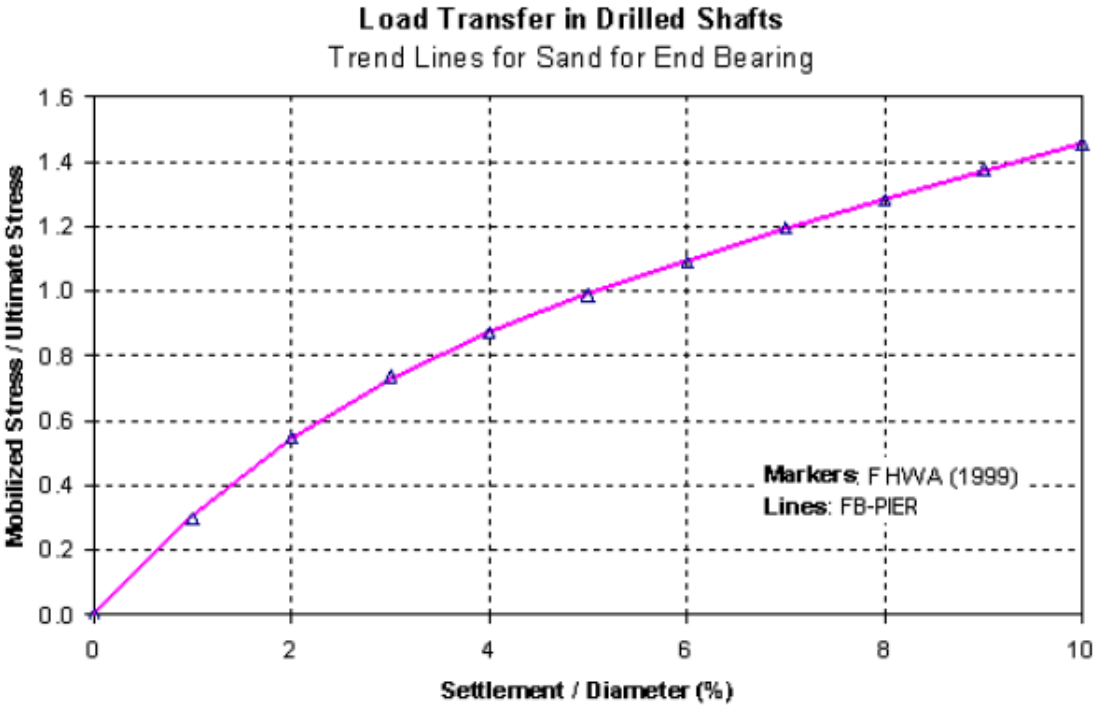

Figure 9: End Bearing for Drilled Shafts in Sand
(Bridge Software Institute)

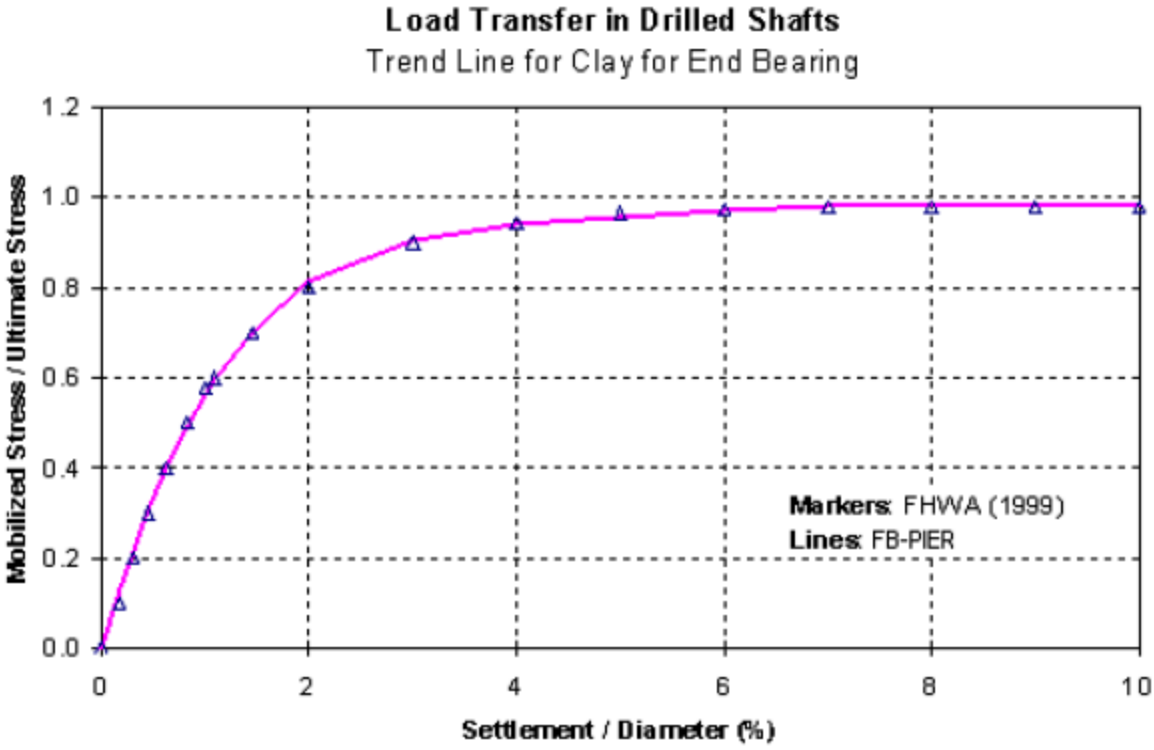

Figure 10: End Bearing for Drilled Shafts in Clay
(Bridge Software Institute)

For modeling drilled shafts in intermediate geomaterial, the user will need to provide many parameters including number of layers, type of surface, drilled shaft diameter, Young's modulus of the drilled shaft, as well as soil and concrete parameters. Finally, the user can choose to input a custom data set of ten points of a Q-Z curve to create a better model.

There also exists an option for the user to input soil properties for dynamic analysis; however, these parameters will only be used in dynamic analysis and for lateral behavior only.

Spring Stiffness

By default, FB-Multipier will include a soil behavior option in the analysis tab. If the user prefers not to use this option, then they will have to enter the pile tip spring stiffness in order to restrain the model. Springs are modeled under "Pier Data" in the Model Data tab. The stiffness can be altered in the x, y, and z directions for both translational and rotational springs. In order to place them on the model, the user will have to select at which nodes or pile cap thath they want the springs to be modeled in the 3D view. FB-Multipier recommends that high spring values be used in order to model a rigid connection.

References

Alonso, E.E. & Olivella, S. (2006). Unsaturated Soil Mechanics Applied to Geotechnical Problems. *Unsaturated Soils,* 1-35.

Bridge Software Institute. (2011). *Bridge Software Insititute.* Retrieved from https://bsi.ce.ufl.edu/.

Hoit, Marc, Ph.D., Chung, Jae H., Wasman, Scott J. , Bollmann, Henry T. (2007). *Development of API Soil Models for Studying Soil-Pile Interaction Analysis Using FB-Multipier*. Gainesville, FL: Bridge Software Institute.

Holtz, R.D., Kovacs, W.D., Sheahan, T.C. (2011). *An Introduction to Geotechnical Engineering.* (2nd ed.) Upper Saddle River, NJ: Pearson Education, Inc.

Lu, Ning, Godt, Jonathan W., & Wu, David T. (2010) A closed-form equation for effective stress in unsaturated soil. *Water Resources Research, Vol. 46*, 1-14.

Lu, Ning & Likos, William J. (2004). *Unsaturated Soil Mechanics*. Hoboken, New Jersey: John Wiley & Sons, Inc.

Lu, Ning & Likos, William J. (2006). Suction Stress Characteristic Curve for Unsaturated Soil. *ASCE Journal of Geotechnical and Geoenvironmental Engineering,* 131-142.

McVay,M. C., Niraula, L. (2004). *Development of Modified T-Z Curves for Large Diameter Piles/Drilled Shafts in Limestone for FB-Pier*. Report Number 4910-4504-878-12, National Technical Information Service, Springfield, VA.

Salgado, Rodrigo. (2008). *The Engineering of Foundations.* New York: McGraw-Hill.

The Engineering Toolbox. (2014). *Area Moment of Inertia*. Retrieved from http://www.engineeringtoolbox.com/area-moment-inertia-d_1328.html.